energies

Article

Time Effect of Water Injection on the Mechanical Properties of Coal and Its Application in Rockburst Prevention in Mining

Xiaofei Liu [1,2,*], Guang Xu [3], Chong Zhang [1,2], Biao Kong [2], Jifa Qian [1], Dong Zhu [2] and Mingyao Wei [4]

1 Key Laboratory of Gas and Fire Control for Coal Mines (China University of Mining and Technology), Ministry of Education, Xuzhou 221116, China; zhangchong@cumt.edu.cn (C.Z.); keenqian@163.com (J.Q.)
2 School of Safety Engineering, China University of Mining and Technology, Xuzhou 221116, China; kongbiao8807@163.com (B.K.); zhudong163@163.com (D.Z.)
3 Department of Mining Engineering and Metallurgical Engineering, Western Australian School of Mines, Curtin University, Kalgoorlie, WA 6430, Australia; guang.xu@curtin.edu.au
4 Institute of Rock and Soil Mechanic, Chinese Academy of Sciences, Wuhan 430071, China; cumtwmy@sina.com
* Correspondence: liuxiaofei@cumt.edu.cn; Tel.: +86-516-8388-4695

Received: 4 September 2017; Accepted: 31 October 2017; Published: 6 November 2017

Abstract: Coal seam water injection is widely used to prevent rockbursts in coal mines, and the duration of water injection is an important parameter related to the effectiveness of rockburst prevention, making it of practical importance to optimize the effective water injection duration. This paper presents the test results of the mechanical properties and pore structure of samples with different soaking time, obtained from a working face where rockburst occurred. Soaking time changes the mechanical properties of samples, and this time effect differs with the coal size (from centimeter to nanometer size). Results of numerical simulation and on-site tests in the Changgouyu coal mine demonstrated that water injection can effectively soften coal bodies and release or transfer stresses, and the time effect of water injection on rock prevention and control is apparent.

Keywords: coal seam water injection; rockburst; soaking test; porosity; numerical simulation; on-site test; time effect

1. Introduction

Coal mine rockbursts in a coal mine are nonlinear dynamic processes. They start with the deformation of coal and rocks caused by mining. Such deformations steadily accumulate energy, and eventually the energy is released suddenly [1,2]. With the increase of mining depth and production, dynamical disasters in coal mines are becoming more serious and frequent, and their intensity is growing, which seriously threatens mining safety [3,4].

Mining optimization design [5,6], regional hazard prevention [7,8], supporting intensity increases or support pattern improvements [9,10] can be used to prevent and control rockbursts in coal mines. The regional hazard prevention method is widely used to prevent rockbursts to eliminate high stress concentrations and weaken the elastic energy accumulation through modifying the properties of coal and rocks. Such methods include coal seam blasting [11], coal seam water injection [12], drill hole pressure relief [13] and directional hydraulic water fracturing [14].

Coal seam water injection can change the bursting liability of coal or rock and reduce or eliminate rockburst disasters in the mining field. It is characterized by a simple operation process, small investment and other favorable features [15]. At present, it is widely used to prevent and control rockburst disasters in China [16,17]. The bursting liability of coal seams is closely related to their water content [18], and the structure and mechanical properties of coal will be changed by the physical-chemical function of water. As the water content of coal increases, the uniaxial compressive strength, peak stress in the stress-strain curve and E of coal decrease and the Poisson's ratio increases [19,20]. The bursting liability of coal weakens with the increase of soak time [21]. The coal seam water injection method is widely applied on site, but it is not necessarily effective in all situations. The properties of coal and rock [22] and the parameters of water injection, including the hole spacing, water flooding pressure and other factors, can affect its effectiveness. In fact, there is a time effect for coal seam water injection. The structure and mechanical properties of coal show obviously differences after different soak times. As soak time increases, those differences become more apparent. Therefore, the time effect of coal seam water injection is of significant importance in its parameter design and effectiveness evaluation. The above researches focused on the mechanic mechanism of water injection into coal on a macro scale (from centimeter to meter size), but there is little research related to this matter on the micro scale. The scanning electron microscope (SEM) technology [23] and the porosity testing technology are helpful to analyze the mechanics mechanism on the micro scale of water injection into coal.

In order to explore the time effect mechanism of water on different sizes of coal (from meter to nanometer size), our study conducted experiments and analyzed the changing law of coal compressive strength, Protodyakonov coefficient, porosity and microstructure of coal samples. By using FLAC-3D, the effect of water injection duration on the effectiveness of rockburst elimination was studied. Based on on-site conditions, an optimized scheme with appropriate parameters was proposed to implement the coal seam water injection method.

2. Experimental Preparation

2.1. Coal Samples Preparation

The coal samples were taken from the No. 9 working face of the Changgouyu coal mine in Beijing, which was a bursting mine. To avoid the anisotropy and heterogeneity and ensure experimental reliability and comparability, three large and complete coal blocks from the same position of the working face were chosen. A vertical drilling machine was used to get Φ50 mm coal core logs from these coal blocks, and they were cut into 100 mm long pieces for test. After that, these coal samples (Φ50 mm × 100 mm) were polished and placed into a drying oven for storage. The sample preparation procedure is shown in Figure 1.

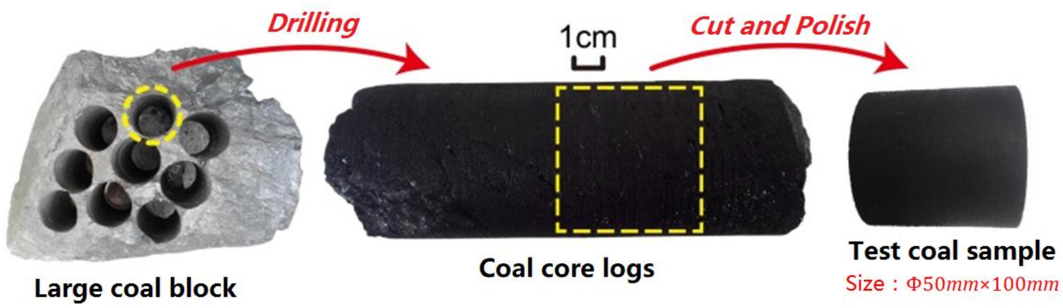

Figure 1. Samples preparation procedure.

The samples were placed into a water container and the initial height of water was set to 1/4 of the sample height. The height of water was increased 1/4 of the coal sample height after each 2 h, thus the coal samples were totally immersed in water after 6 h. Samples were taken out from water at the fifth day, tenth day and fifteenth day for testing.

2.2. Experimental Devices and Procedures

The mechanical parameters of the coal samples under different soak time were tested. The tested parameters include uniaxial compressive strength, Protodyakonov coefficient, porosity, pore volume, pore surface area and micro structure:

(1) The water content and absorption, the uniaxial compressive strength and Protodyakonov coefficient were tested according to the China GB/T23561 national standard. The size of samples in the uniaxial compressive strength test is Φ50 mm × 100 mm. The grain size of samples in the Protodyakonov coefficient test is less than 20 mm.

(2) The pore parameters of coal were measured by the 9310 mercury pressure microporous structure tester manufactured by Micromeritics (Micromeritics Instrument Corporation, Norcross, GA, USA). The porosity, pore volume and pore surface area of the samples were tested after soaking for 5 days, 10 days and 15 days.

(3) The microstructure and morphology of coal were observed by an S-3000N scanning electron microscope (Hitachi, Ltd., Tokyo, Japan). The sample size was 10 mm × 10 mm × 10 mm. Before testing, the conductivity of samples was treated by the ion sputtering method and the thickness of the gold plating layer was controlled at 5~10 nm.

3. Experimental Results Analysis

3.1. Compressive Strength

After soaking, the uniaxial compressive strength of the coal decreases with the increase of soaking duration. The overall decrease trend can be fitted to a cubic polynomial equation (Figure 2a). When the soaking time was 5 days, its decrease was largest, from 25.44 MPa to 13.63 MPa. With time increase, the decrease range was smaller after another five days, from 13.63 MPa to 12.42 MPa. After the third five days, the decrease range became bigger, from 12.42 MPa to 8.13 MPa. Therefore, the first five days of soaking are the most effective in changing the compressive strength of coal sample, and its relative reduction per day reaches to 2.36 MPa. The natural water content of the coal sample is 0.26%, and the average water content exceeded 1.29% after soaking. With such a higher water absorption value, the application of water injection is feasible.

3.2. Protodyakonov Coefficient

The original test data is shown in Table 1.

Table 1. Test results of Protodyakonov coefficient.

Coal Sample	Serial Number	Number of Hits n	Height of Coal Dust l (mm)	Protodyakonov Coefficient f	Average Value
Original sample	1	3	46.5	1.2903	1.33
	2	3	45.5	1.3187	
	3	3	43.5	1.3793	
Soaking 5 days	1	3	49.0	1.2245	1.26
	2	3	47.5	1.2632	
	3	3	45.5	1.3187	
Soaking 10 days	1	3	67.5	0.8877	0.87
	2	3	68.0	0.8824	
	3	3	69.5	0.8633	
Soaking 15 days	1	3	78.5	0.7643	0.76
	2	3	79.5	0.7547	
	3	3	77.5	0.7742	

The Protodyakonov coefficient of coal sample is calculated according to Equation (1):

$$f = \frac{20n}{l} \quad (1)$$

where: f is Protodyakonov coefficient, n is the number of hits during a test, and l is the height of coal dust from coal sample after hits in a test.

As soak duration increases, the Protodyakonov coefficient gradually decreases and there is a linear relationship between them (Figure 2b). After soaking for five days, there is point of change for the Protodyakonov coefficient, where it rapidly decreases. After soaking for 10 days, the decrease rate becomes low. Therefore the soaking duration between five days and 10 days is the most effective timing in reducing the Protodyakonov coefficient.

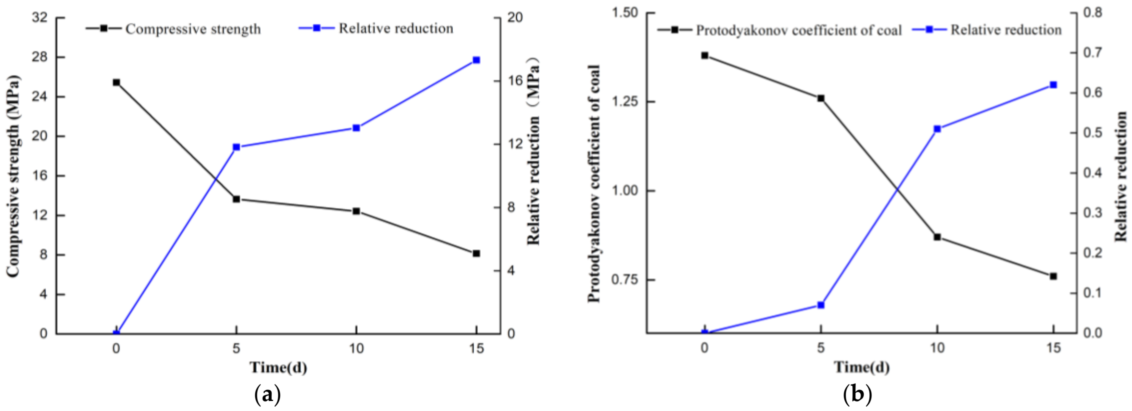

Figure 2. The change of mechanical parameters of coal with soaking duration: (**a**) compressive strength and (**b**) Protodyakonov coefficient.

3.3. Pore Structure

3.3.1. Relationship between Porosity and Soaking Duration

It can be seen in Table 2 that for different soaking durations, there is obvious changes of true specific gravity, apparent specific gravity and porosity. The longer the soaking duration is, the bigger porosity is. When the soaking duration is between five days and 10 days, the rate of porosity increase is the maximum, and its relative increment per day reaches to 0.316. After 10 days, the increase rate becomes low.

Table 2. Test results of specific gravity and porosity of coal samples.

Coal Sample	True Specific Gravity (g/cm^3)	Apparent Specific Gravity (g/cm^3)	Porosity (%)	Increment of Porosity (%)		Reduction of Compressive Strength (MPa)	
				Total Increment	Relative Increment Per Day	Total Reduction	Relative Reduction Per Day
Original sample	1.6475	1.6739	2.64	-	-	-	-
Soaking 5 days	1.5762	1.6425	4.21	1.57	0.314	11.81	2.36
Soaking 10 days	1.6134	1.7058	5.79	3.15	0.316	3.15	0.63
Soaking 15 days	1.5961	1.7027	6.68	4.04	0.178	4.29	0.86

3.3.2. Relationship between Pore Volume and Soaking Duration

Table 3 shows the common method of pore classification in the coal industry in China, which is on the basis of the diameter ranges of pore in the coal body. The Chinese names of different types of pore are translated as microspore, minor mesopore, mesopore and macrospore in this paper, and they are completely different with the diameter classification by the International Union of Pure and Applied

Chemistry. They are commonly called diffusion pore, slight permeation pore and strong permeation pore [24].

Table 4 shows coal samples' pore volume and its percentage of all types of pore for different soaking durations. The total pore volume, all types of pore volume and their percentage increase with soaking time. As shown in Figure 3, the 5th day is a changing point after which time coal pore volume increases rapidly. When soaking duration is between 5 days and 10 days, the volume increase of total pore, micropore, minor mesopore, macrospore and visible pore are the maximum. This indicates the internal structure of coal changes dramatically during this period.

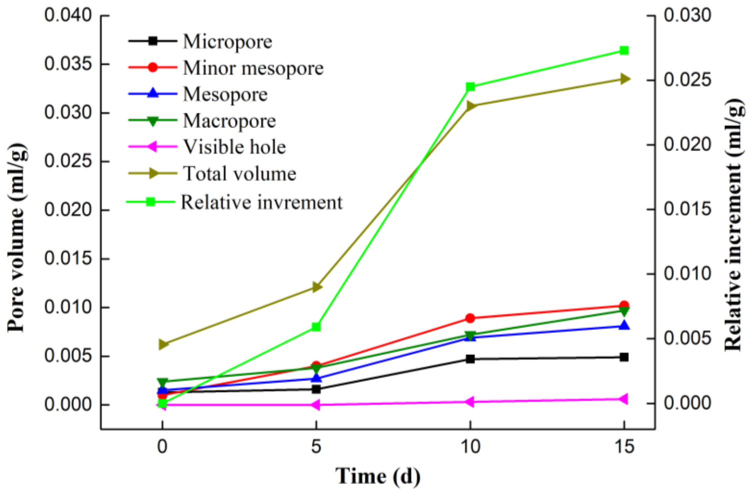

Figure 3. Curves of all types of pore volume of coal samples before and after soaking.

3.3.3. Relationship between Pore Surface Area and Soaking Duration

The pore surface area and its percentage during different soaking time are shown in Table 5. It can be seen that micropore and minor mesopore have large pore surface area, and mesopore and macrospore are relatively small. Therefore, the total pore surface area is mainly composed of micropore and minor mesopore. As soaking time increases, the surface area of all types of coal pores increases, and the increase of micropore surface area is the most significant. When the soaking time is 10 days, the increase of total pores surface area reaches a maximum (as shown in Figure 4). The larger pore surface area is, the more easily the samples are broken under the same loading conditions. Due to soaking, coal pore surface area is changed that makes the strength of coal internal structure reduce.

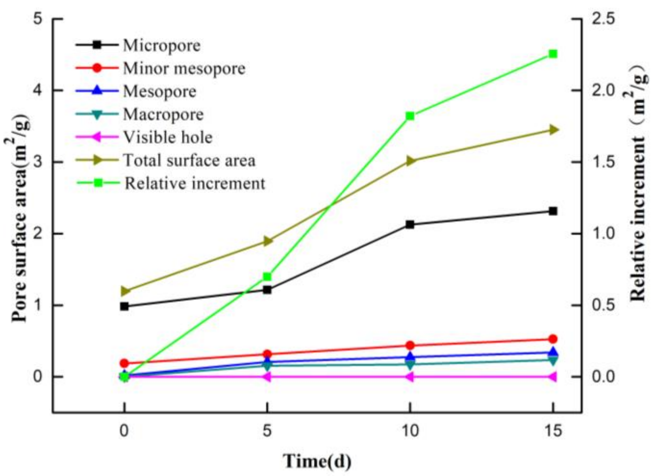

Figure 4. Curves of the change of pore surface area with soaking time.

Table 3. The common method of pore classification of coal in China.

Size	Type of Pore			
	Microspore	Minor Mesopore (Diffusion Pore)	Mesopore (Slight Permeation Pore)	Macrospore (Strong Permeation Pore)
Diameter (nm)	<10	10~100	100~1000	>1000

Table 4. The distribution of pore volume of coal samples.

Coal Sample	Microspore		Minor Mesopore		Mesopore		Macrospore		Visible Pore		Adsorption Volume (mL/g)	Permeation Volume (mL/g)	Total Volume (mL/g)
	Volume (mL/g)	Percentage (%)	Volume (mL/g)	Percentage (%)	Volume (mL/g)	Percentage (%)	Volume (mL/g)	Percentage (%)	Volume (mL/g)	Percentage (%)			
Original sample	0.0013	20.97	0.0010	16.13	0.0015	24.19	0.0024	38.71	0.0000	0.00	0.0013	0.0049	0.0062
Soaking 5 days	0.0016	13.23	0.0040	33.06	0.0027	22.31	0.0038	31.40	0.0000	0.00	0.0016	0.0105	0.0121
Soaking 10 days	0.0047	15.31	0.0089	28.99	0.0069	22.48	0.0072	23.45	0.0003	0.98	0.0047	0.0026	0.0307
Soaking 15 days	0.0049	14.63	0.0102	30.45	0.0081	24.18	0.0097	28.96	0.0006	1.79	0.0049	0.0286	0.0335

Table 5. The distribution of pore surface area of coal samples.

Coal Sample	Microspore		Minor Mesopore		Mesopore		Macrospore		Visible Pore		Total Surface Area (m^2/g)
	Surface Area (m^2/g)	Percentage (%)	Surface Area (m^2/g)	Percentage (%)	Surface Area (m^2/g)	Percentage (%)	Surface Area (m^2/g)	Percentage (%)	Surface Area (m^2/g)	Percentage (%)	
Original Sample	0.984	82.27	0.188	15.72	0.019	1.59	0.005	0.42	0.0000	0.00	1.196
Soaking 5 Days	1.215	64.12	0.315	16.62	0.207	10.92	0.155	8.18	0.0003	0.16	1.895
Soaking 10 Days	2.125	70.43	0.437	14.48	0.276	9.15	0.174	5.77	0.0005	0.17	3.017
Soaking 15 Days	2.314	65.33	0.527	15.27	0.341	9.88	0.237	6.69	0.0006	0.17	3.452

3.4. Microstructure

Based on the SEM results, the microstructure and morphology of coal samples before and after different soaking time were as observed in Figures 5–9.

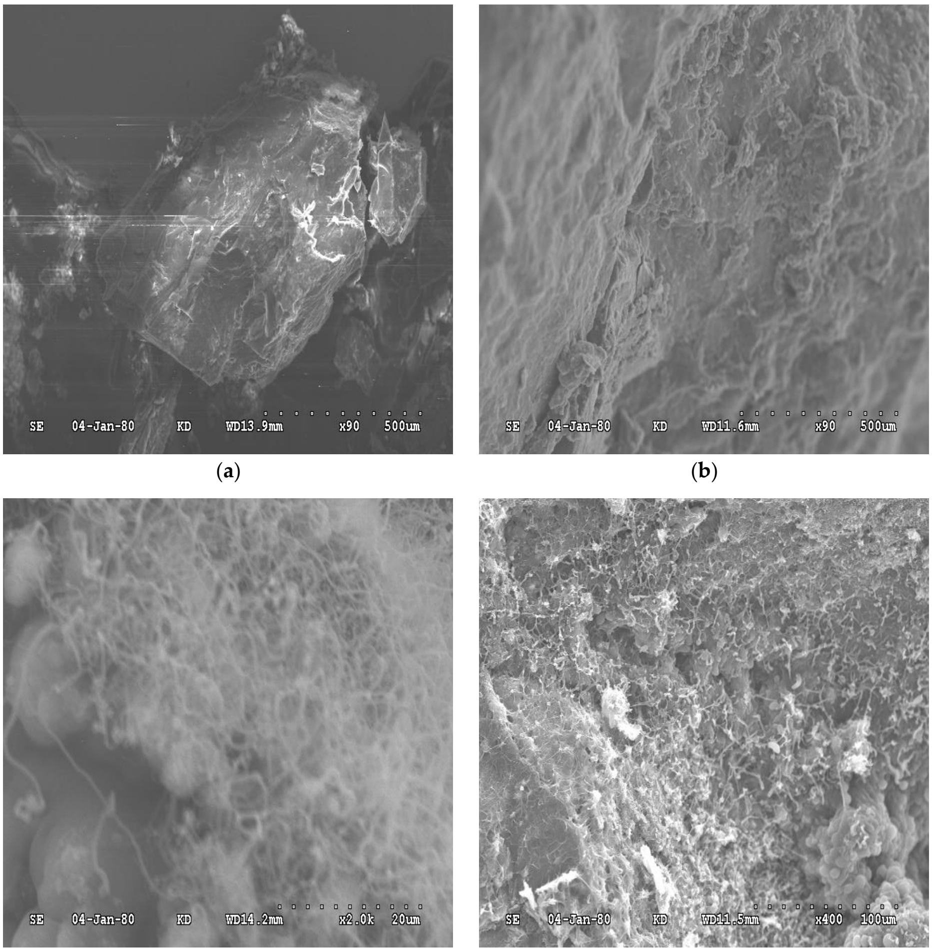

(**a**) (**b**) (**c**) (**d**)

Figure 5. SEM image for the overall structure change: (**a**) before soaking; (**b**) soaking for 5 days; (**c**) soaking for 10 days and (**d**) soaking for 15 days.

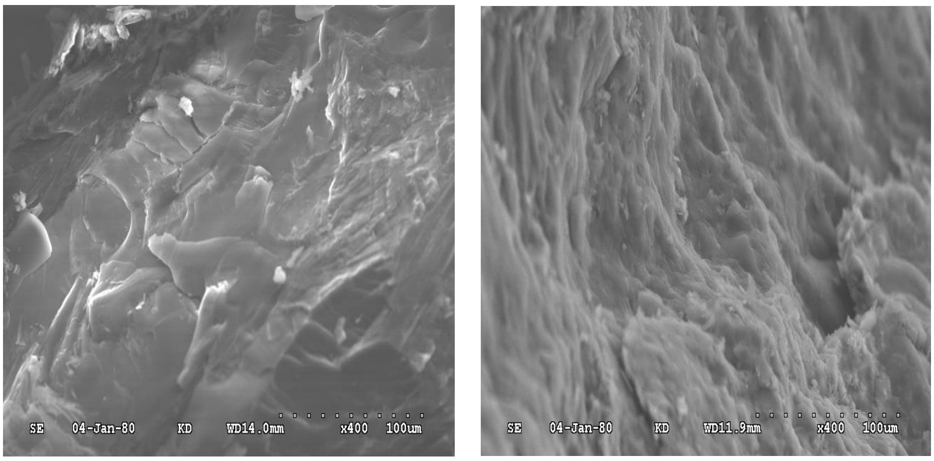

(**a**) (**b**)

Figure 6. *Cont.*

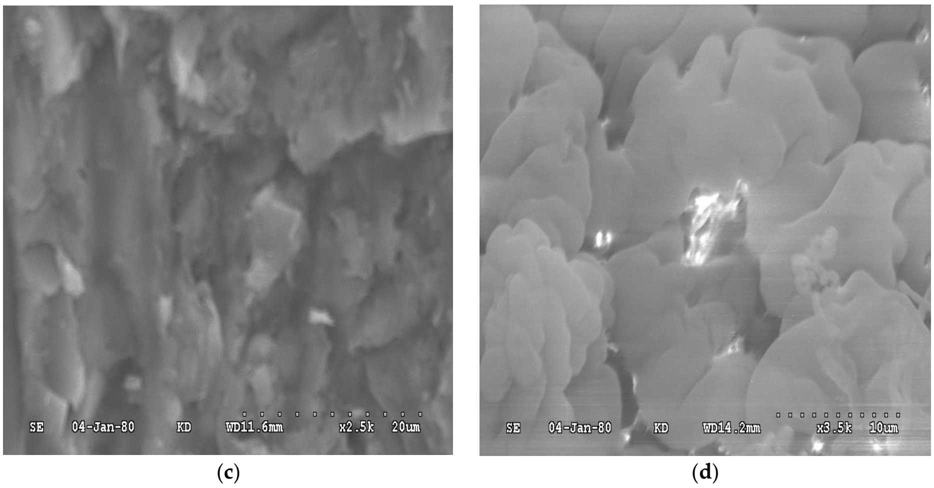

(**c**) (**d**)

Figure 6. SEM image of the internal flake structure: (**a**) before soaking; (**b**) soaking for 5 days; (**c**) soaking for 10 days and (**d**) soaking for 15 days.

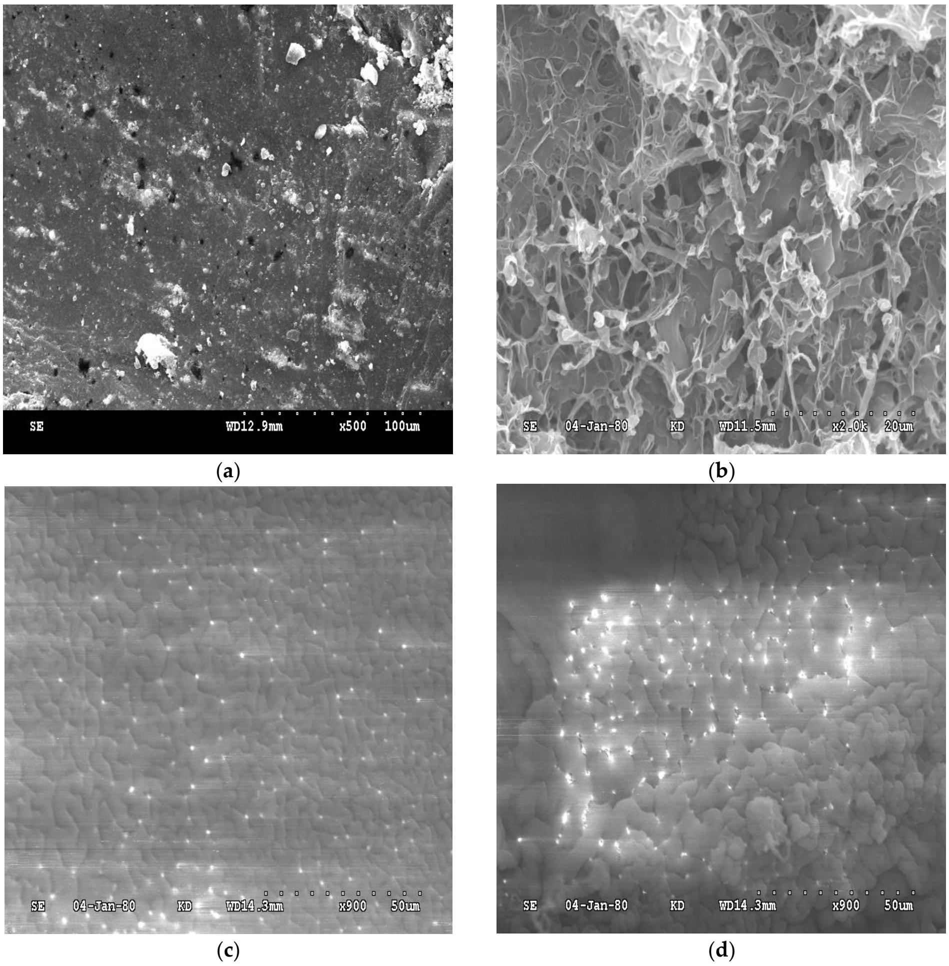

Figure 7. SEM image of the internal pore structure: (**a**) before soaking; (**b**) soaking for 5 days; (**c**) soaking for 10 days and (**d**) soaking for 15 days.

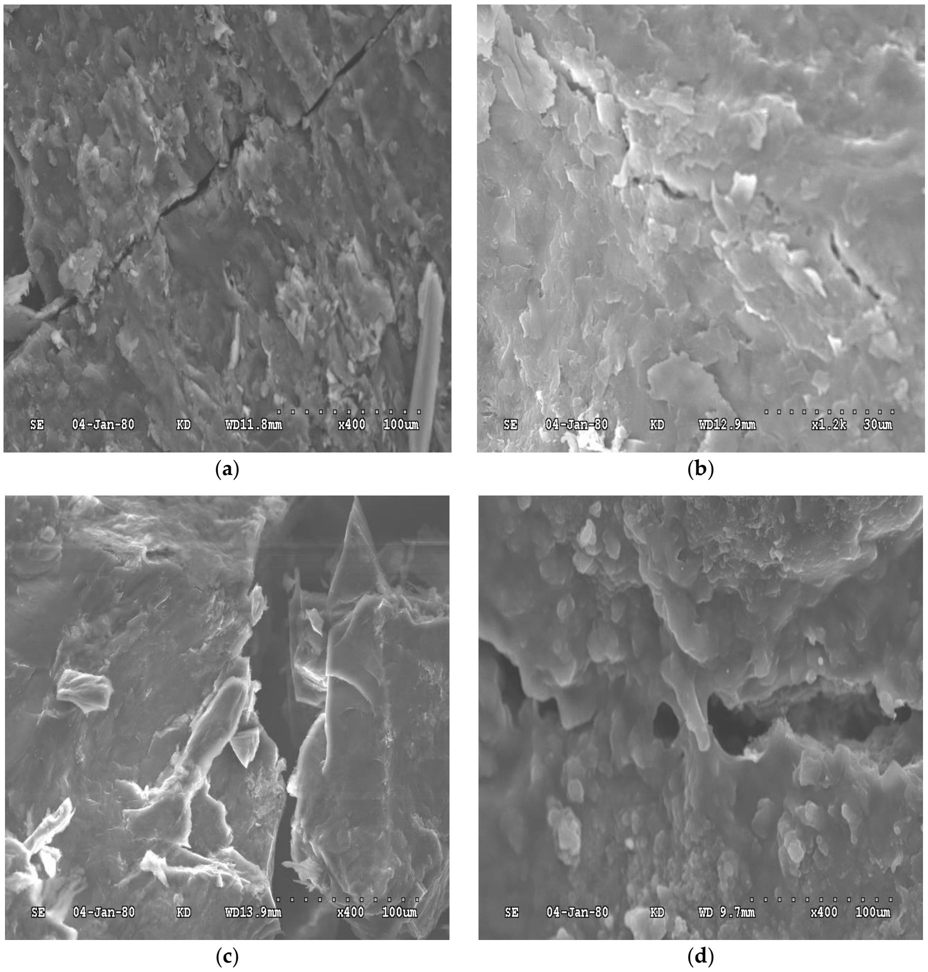

Figure 8. SEM image of the internal cracks structure: (**a**) before soaking; (**b**) soaking for 5 days; (**c**) soaking for 10 days and (**d**) soaking for 15 days.

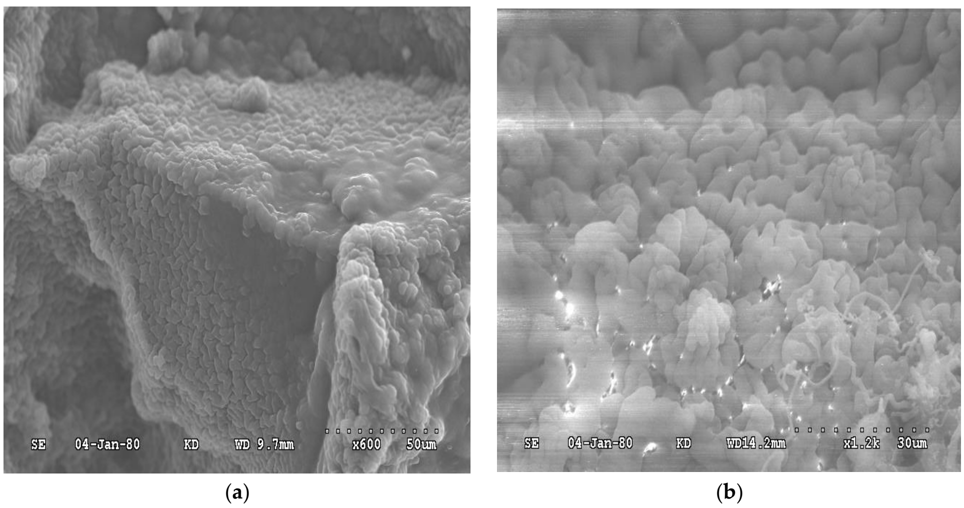

Figure 9. SEM image of the fold structure: (**a**) before soaking and (**b**) soaking for 15 days.

From the SEM images, a large number of pores, cracks, and flake structures can be seen inside the coal samples. Before soaking, there is no obvious change on those structures as shown in Figures 5a, 6a, 7a and 8a. From Figure 5, it can be seen that the internal structures of samples are smooth and there are no obvious protuberances. As soaking duration increases, the surface becomes raw and bubble-like structures and cracks start to appear.

Figure 6 shows the flake structure of coal samples. From Figure 6a, it can be seen that the surface of the coal sample is smooth and there is no apparent development of pore and flake structures. The flakes are closely interlaced at the coal surface. As soaking duration increases, flake structures gradually develop and separate from the coal body (as shown in Figure 6b–d). When the soaking time is 15 days, a large number of pores appear in the flake structures, which cause the microstructure surface area to increase.

Figure 7 shows the pore structure of the samples. As can be seen from Figure 7a, only few small pores are scattered on the coal surface. When the soaking duration is five days, filamentous structures and cracks are produced. It can be seen in Figure 7c,d that there are a large number of pores and the surface area increases. Pores are surrounded by fold structures that increase the microstructure surface area.

Figure 8 shows the development of the crack structure. Before soaking, cracks are rigid and their ports are smooth with no adhesive material around. With soaking time increase, there is protruding structure at their ports and a large number of flake structures develop. After soaking for 15 days, glaze structure occurs at crack ports which make the upper and lower of crack surfaces adhere together. This increases crack surface area.

Figure 9 shows the fold structure of coal samples after soaking. When the soaking time is between 10 days and 15 days, folds occur at the surface of organic components in the coal and this causes the microstructure surface area to increase.

In summary, the surface area and total volume of the internal microstructure of coal samples can be greatly increased by soaking. These findings agree with the measurements in Section 3.3. The findings indicate water injection can change the coal microstructure, which makes it favorable for stress release and rockburst disaster prevention and control.

4. Application in Rockburst Prevention

For further studying the time effect of coal seam water injection, this study conducted numerical simulations by using real geological condition data from a mine, and performed on-site tests for validation purposes.

4.1. Numerical Simulation

4.1.1. Model and Parameters

The FLAC-3D software is a professional tool used to simulate the stress and deformation of rock materials under loading conditions [25], and can be used to simulate the water injection process for reducing stress concentration and the danger of rockbursts. The simulated area is based on the conditions of the No. 9 working face in the Changgouyu coal mine where rockbursts have occurred. The model has 156,000 units (Figure 10) and its dimensions are 120 m × 200 m × 140 m. The model boundary is fixed, with the horizontal displacement and the boundary at the bottom is fixed with the vertical displacement. A uniform loading of 12.0 MPa is applied on the top, which is equivalent to the vertical stress of about 500 m rock mass. The initial displacement and its rate are set to be zero, and the original main stress is installed according to the actual ground stress. The Mohr-Coulomb strain softening failure criterion is adopted in the model. The internal friction angle and cohesion softening parameters used for modelling the immediate and main roof are shown in Table 6. Coal bedding is simulated by using the interface unit. The normal stiffness and shear stiffness are both 1.0×10^4 MPa. The physical mechanics parameters of the coal seam and the immediate roof are set according to test results. The parameters of the floor, roof and other strata are listed in Table 7. The upper +150 m level is firstly mined, and the gob area is treated as backfilling with soft rocks with parameters listed in Table 6.

Table 6. The softening parameters of backfilling rocks.

Categories	Immediate Roof				Main Roof			
Strain (ε)	0.00	0.01	0.02	0.50	0.00	0.01	0.02	0.50
Cohesion C/MPa	1.8×10^6	0.9×10^6	0.5×10^6	1.0×10^4	2.0×10^6	1.0×10^6	1.0×10^5	1.0×10^4
Internal Friction Angle	30	25	20	15	33	28	25	22

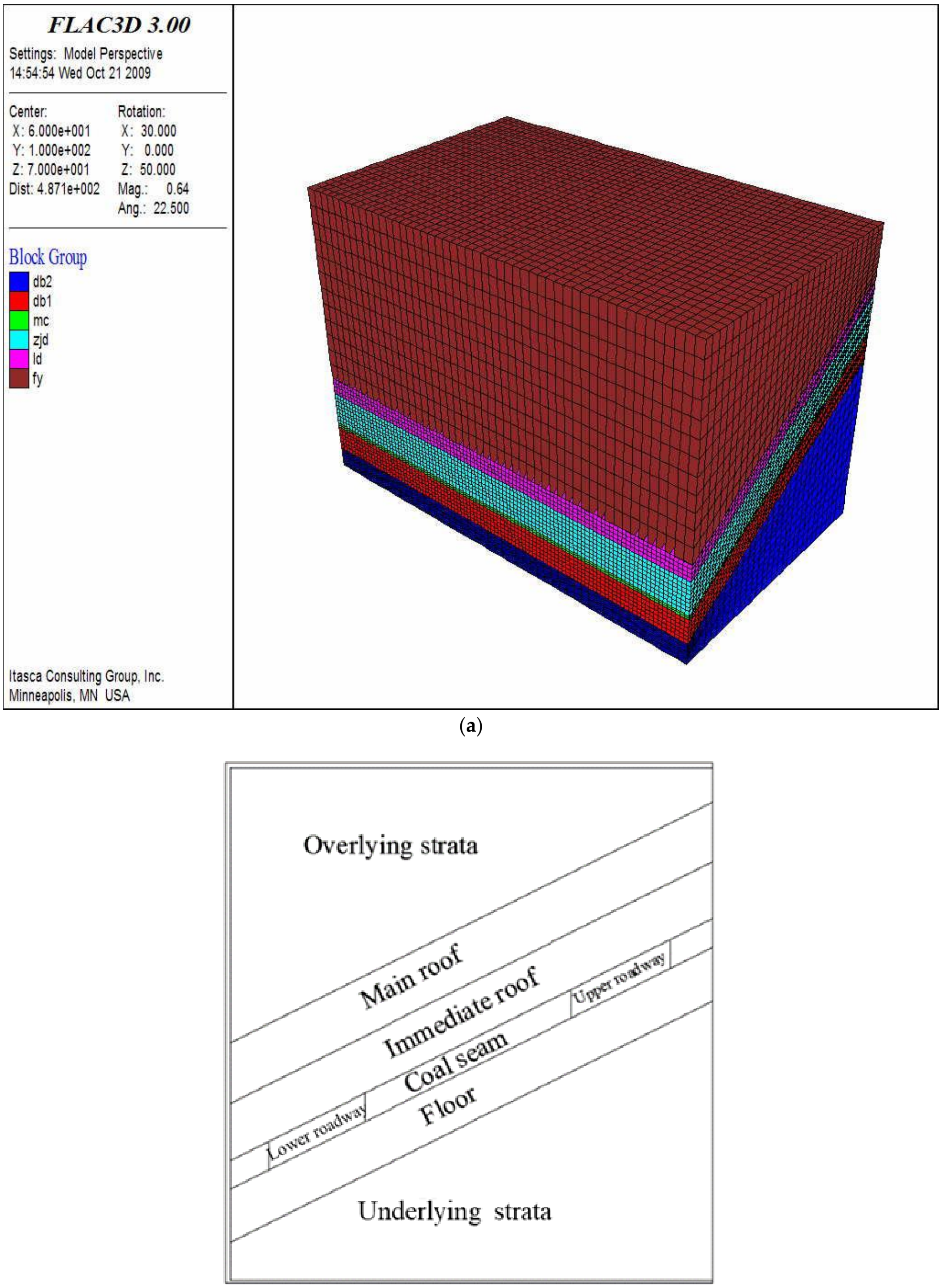

(**a**)

(**b**)

Figure 10. Schematic diagram of the model: (**a**) model mesh and (**b**) overall model structure.

Table 7. Rock mechanic parameters.

Rock Bedding	Bulk Modulus (Gpa)	Shear Modulus (Gpa)	Density (kg·m^{-3})	Friction Angle (°)	Cohesion (Mpa)	Tensile Strength (Mpa)
Overlying strata	2.6	2.4	2500	30	2	2.6
Main roof	3.2	2.4	2700	33	3.5	3.0
Direct roof	2.4	1.8	2600	30	1.8	2.4
Coal seam	1.8	1.4	1400	28	1.3	1.8
Floor	2.0	1.6	2600	28	1.5	2.0
Underlying strata	3.0	2.6	2500	33	2.0	2.6

4.1.2. Water Injection Parameters Optimization

Water injection parameters play an important role in the effectiveness of preventing and controlling rockbursts in coal seams. These parameters include borehole length and diameter, borehole interval, borehole number, and water injection time. Firstly, the water injection effect under different conditions of borehole diameter, length, interval and numbers is simulated in this study. After reasonable values for these parameters are determined, the effect of stress reduction and rockburst prevention under varied water injection times (5, 10, 15 and 30 h) are simulated. The simulation results are shown in Figures 11–15.

The numerical results for different combinations of borehole lengths and borehole diameters are given in Figures 11 and 12. It shows that the water affected area becomes more extensive and the release and transfer of stress concentration are easier with the increase of borehole length and borehole diameter. When using a borehole with length of 60 m and diameter of 60 mm, the stress of coal seam is obviously transferred away from the stress concentration area and the risk of rockburst becomes lower. Based on numerical results and actual mining conditions of the Changgouyu mine, our study can identify that the best borehole length and diameter are 60 m and 60 mm, respectively.

With the 60 m length and 60 mm diameter borehole, the simulation of stress distribution under different borehole intervals are given in Figure 13. It suggests that water injection with 20 m interval has no obvious influence on stress distribution. However, water injection effectiveness is slightly better when the borehole intervals are 10 m and 15 m. Due to the higher cost associated with small borehole intervals, it is reasonable to choose 15 m as the best borehole interval.

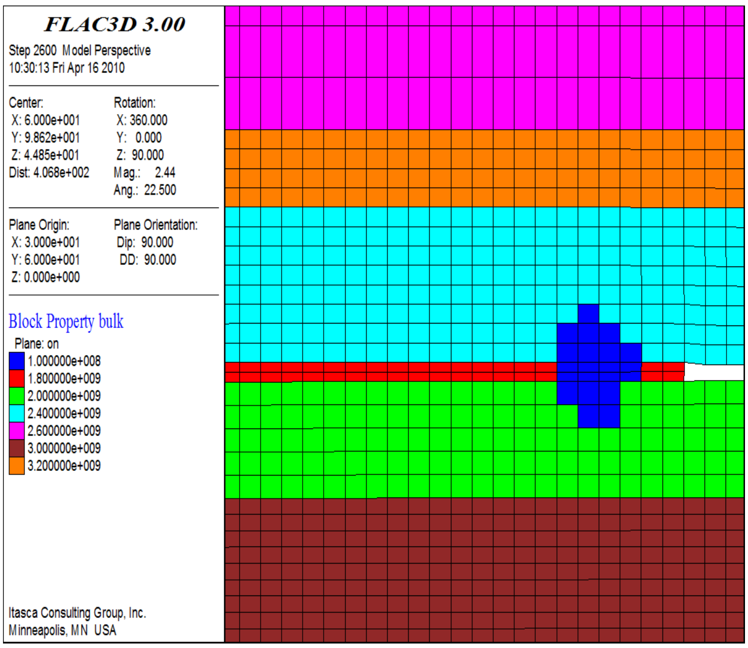

(**a**)

Figure 11. *Cont.*

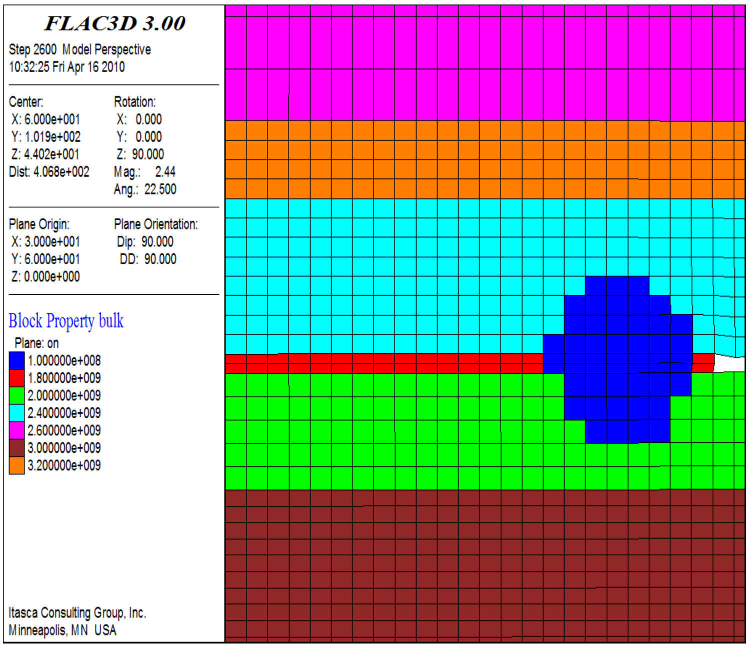

(**b**)

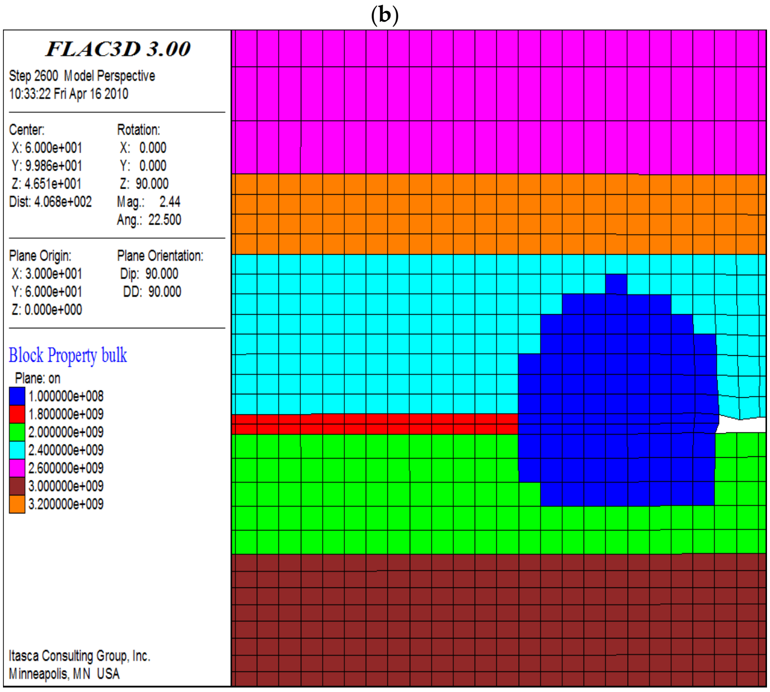

(**c**)

Figure 11. Simulation of water affected area under three different conditions: (**a**) Borehole length 40 m, diameter 50 mm; (**b**) Borehole length 50 m, diameter 55 mm; (**c**) Borehole length 60 m, diameter 60 mm.

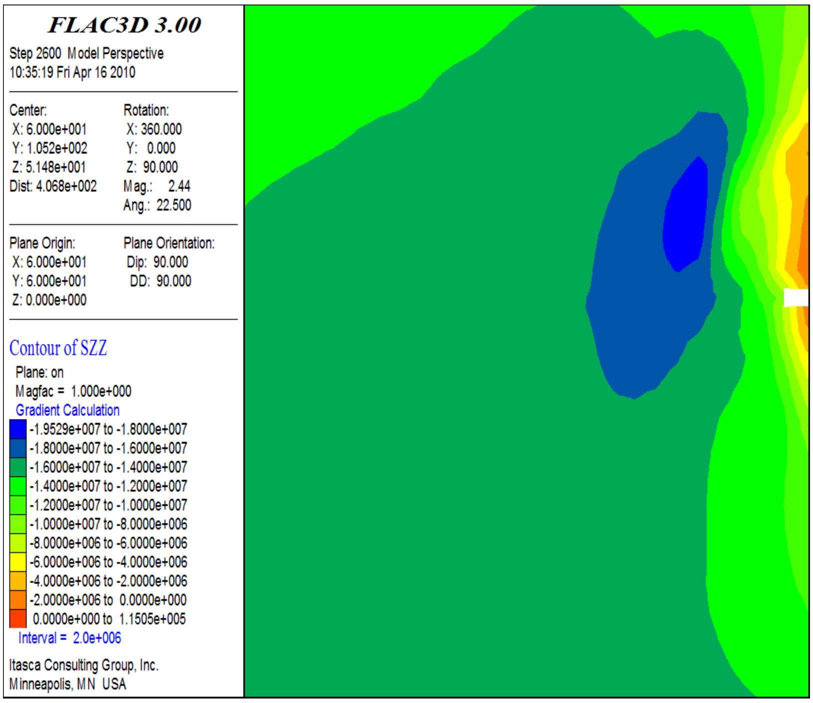

(**a**)

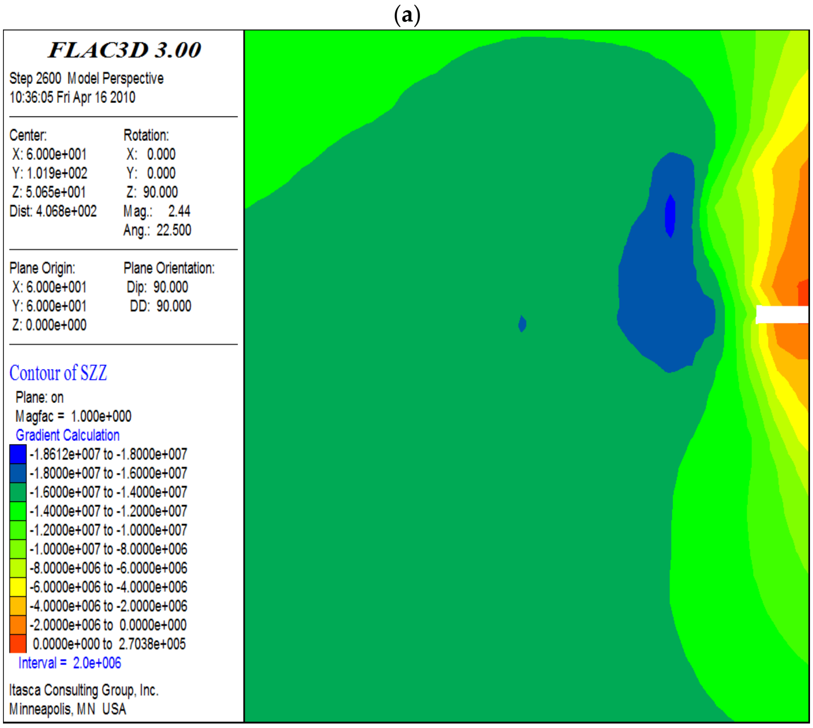

(**b**)

Figure 12. *Cont.*

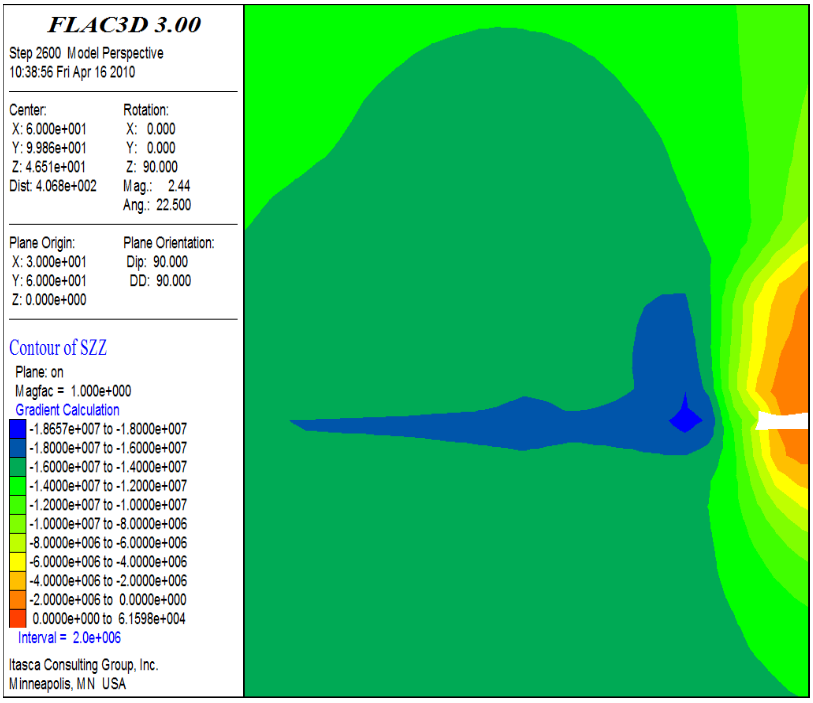

(**c**)

Figure 12. Simulation of stress distribution under three different conditions: (**a**) Borehole length 40 m, diameter 50 mm; (**b**) Borehole length 50 m, diameter 55 mm; (**c**) Borehole length 60 m, diameter 60 mm.

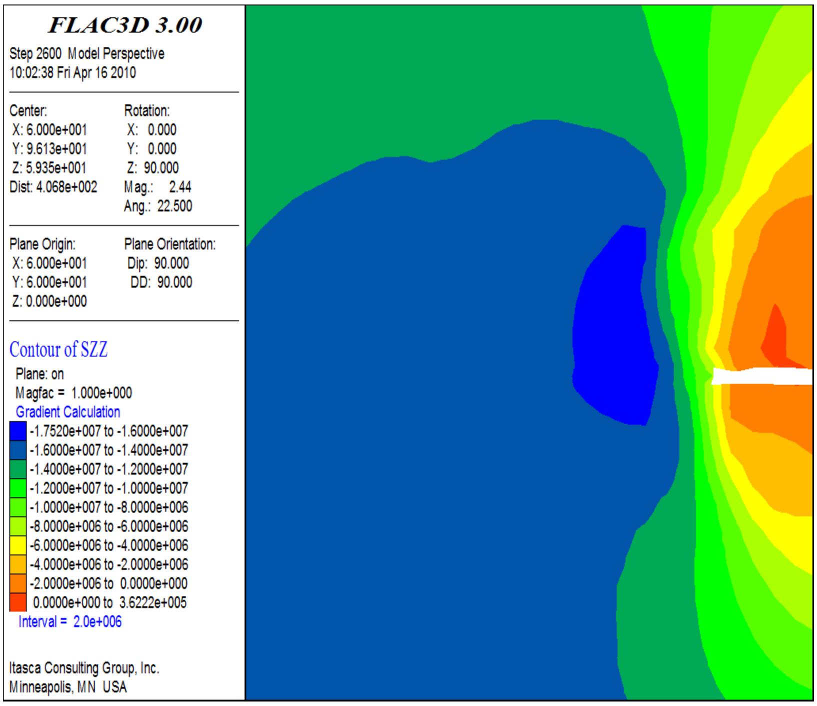

(**a**)

Figure 13. *Cont.*

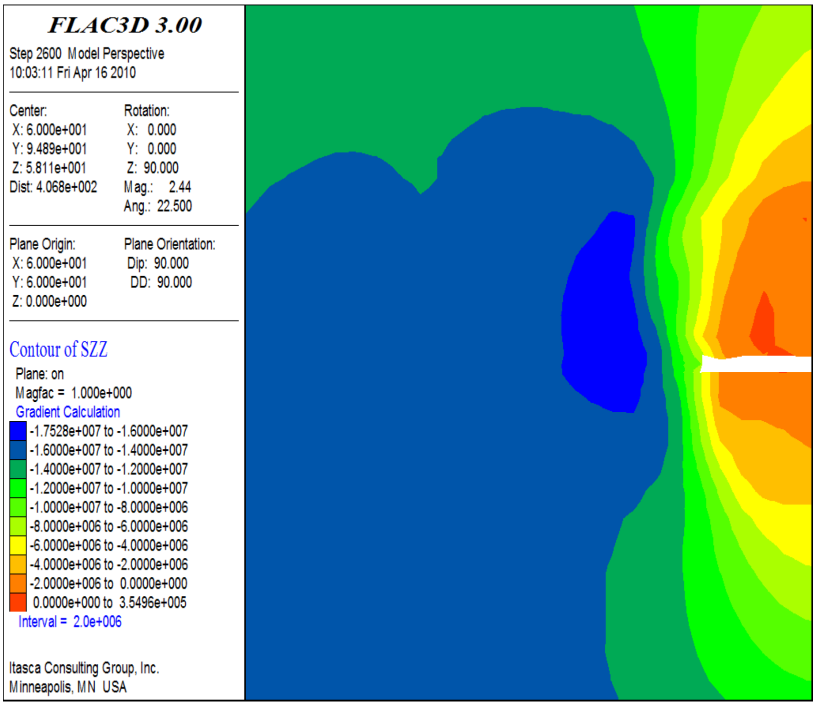

(**b**)

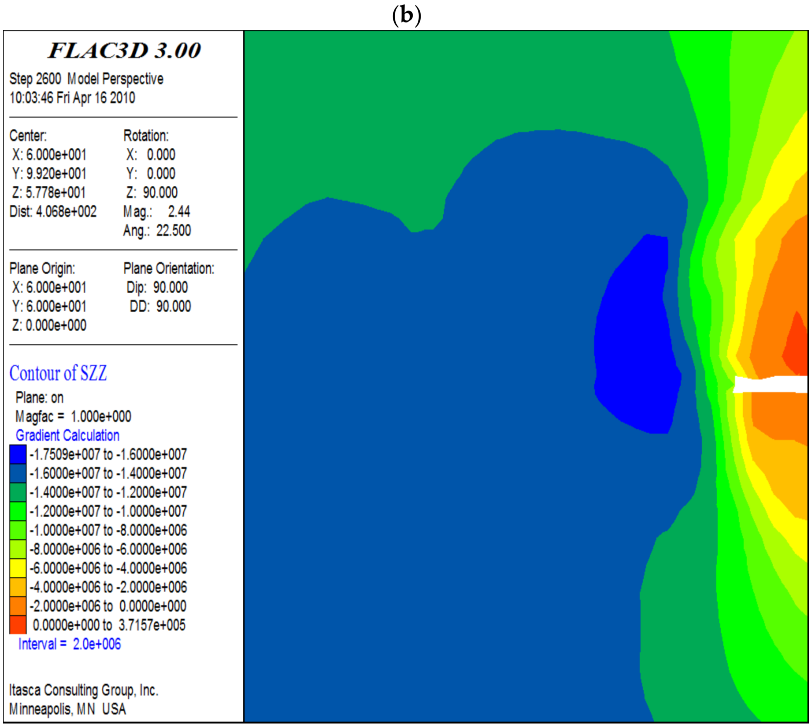

(**c**)

Figure 13. Simulation of stress distribution under three different borehole interval conditions: (**a**) 10 m; (**b**) 15 m; (**c**) 20 m.

With the above determined borehole parameters, the effect of different borehole number (1, 2 or 3 holes injected simultaneously) are simulated and the results are shown in Figures 14 and 15. The effect with three boreholes injecting water simultaneously is far better than that of a single borehole, and the effect of two boreholes is also slightly better than that of a single borehole. It is apparent that more water injection boreholes result in more effective rockburst prevention. However, the construction conditions and the cost should also be considered when determining this parameter.

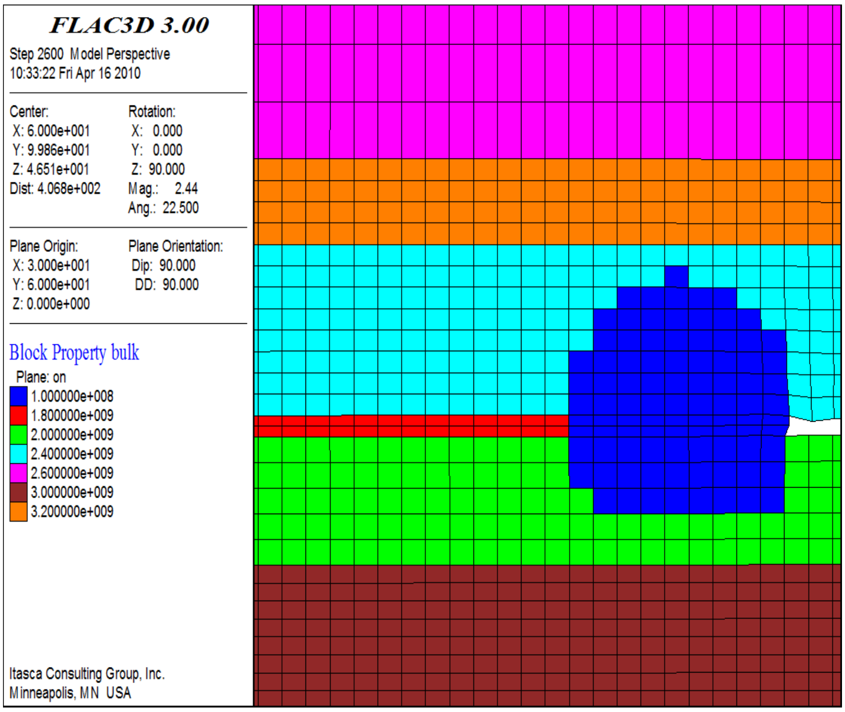

(**a**)

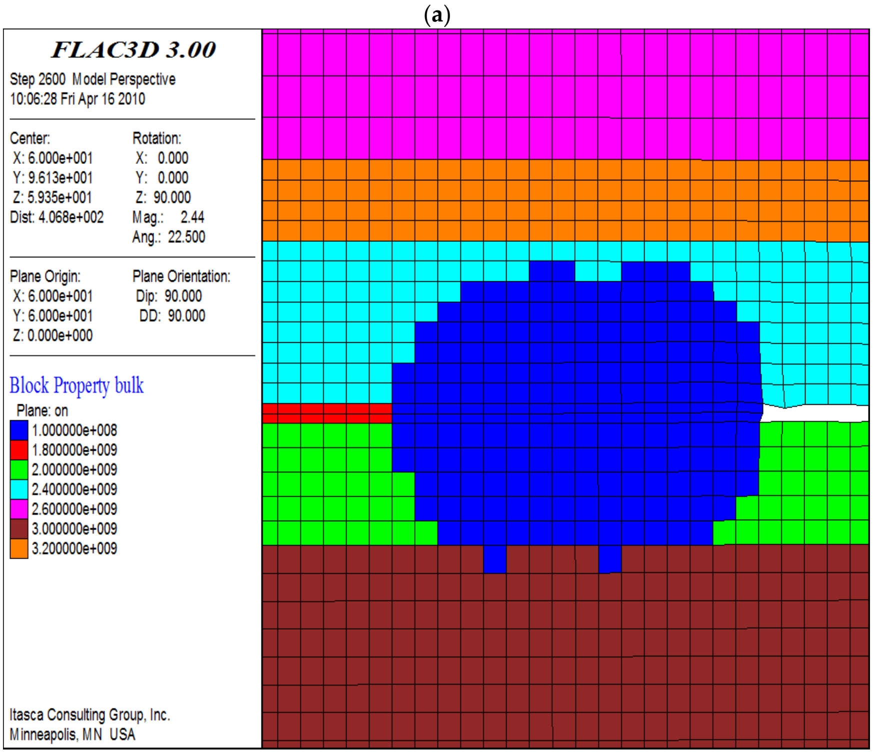

(**b**)

Figure 14. *Cont.*

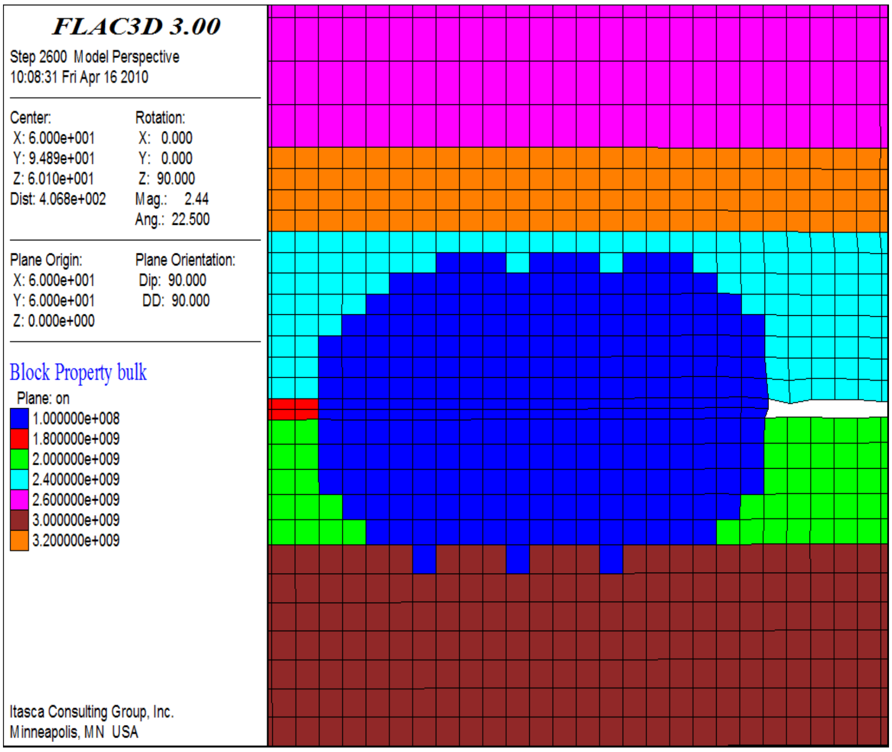

(**c**)

Figure 14. Simulation of the water-affected area for different number of boreholes: (**a**) one, (**b**) two and (**c**) three.

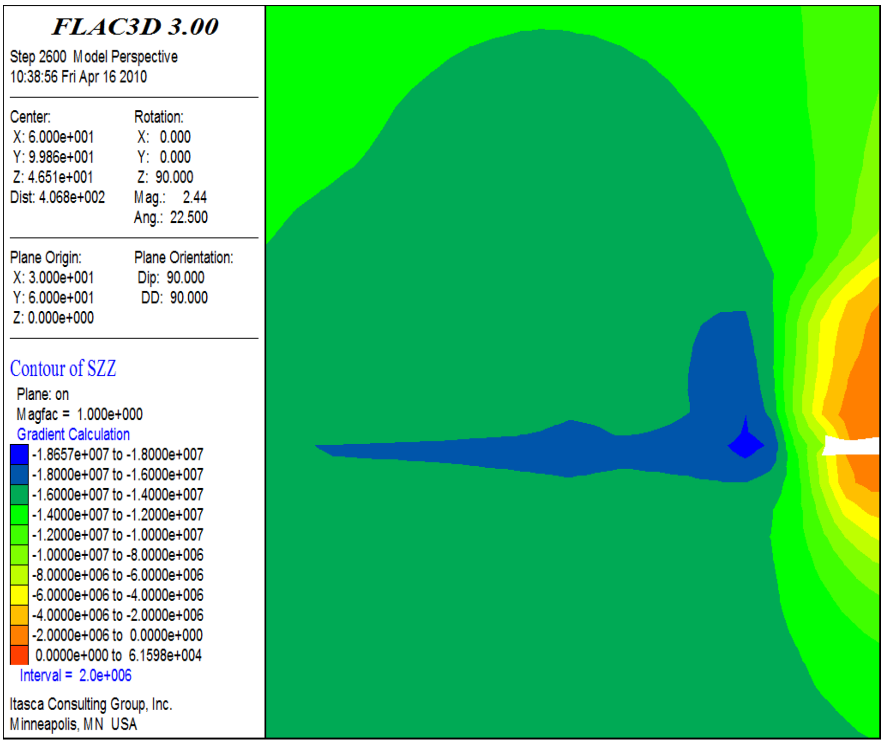

(**a**)

Figure 15. *Cont.*

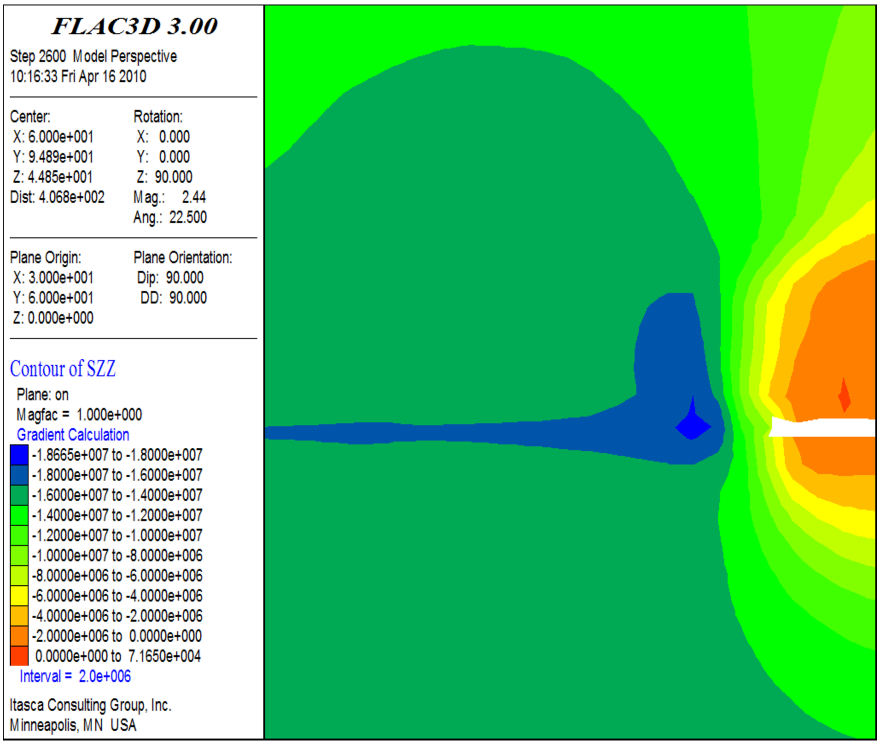

(**b**)

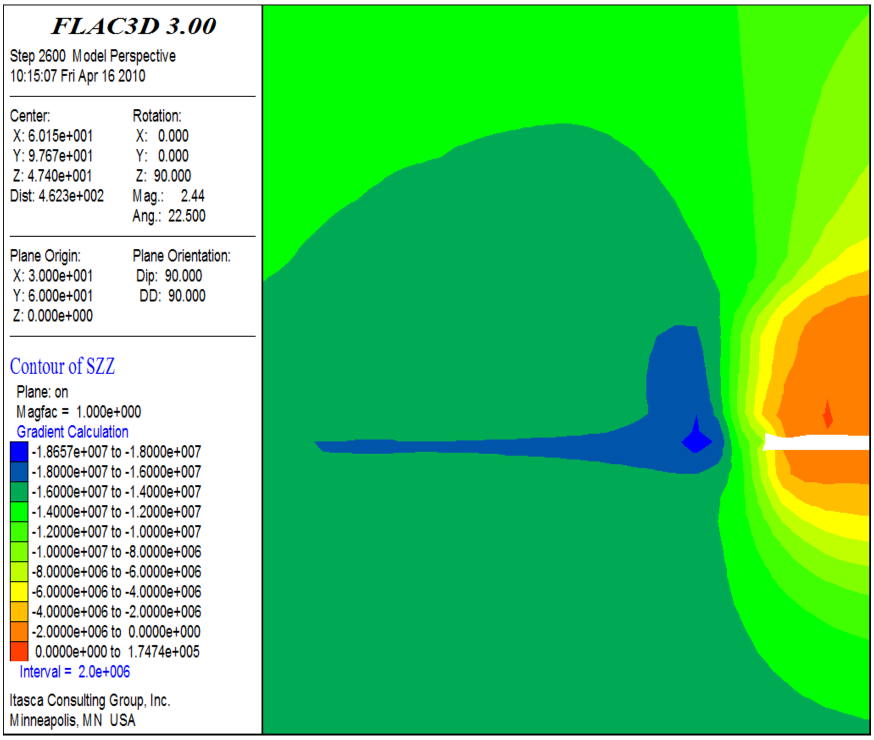

(**c**)

Figure 15. Simulation of stress distribution under different number of boreholes: (**a**) one; (**b**) two and (**c**) three.

4.1.3. Simulation of the Time Effect of Water Injection on Reducing Vertical Stress

Three water injection boreholes, along the coal seam tendency, are drilled in the coal body of the roadway of No. 9 working face. The depth and diameter of each borehole is 60 m and 60 mm.

The space between two adjacent holes is 10 m, with the first one 15 m from the cutting of working face. Water is injected to the three injection boreholes at the same time, and the changes of vertical stress in coal seam are shown in Figure 16. As a result of water injection, coal body is softened and the stress concentration changes significantly. With the duration of water injection increase, the stress concentration is gradually released or transferred.

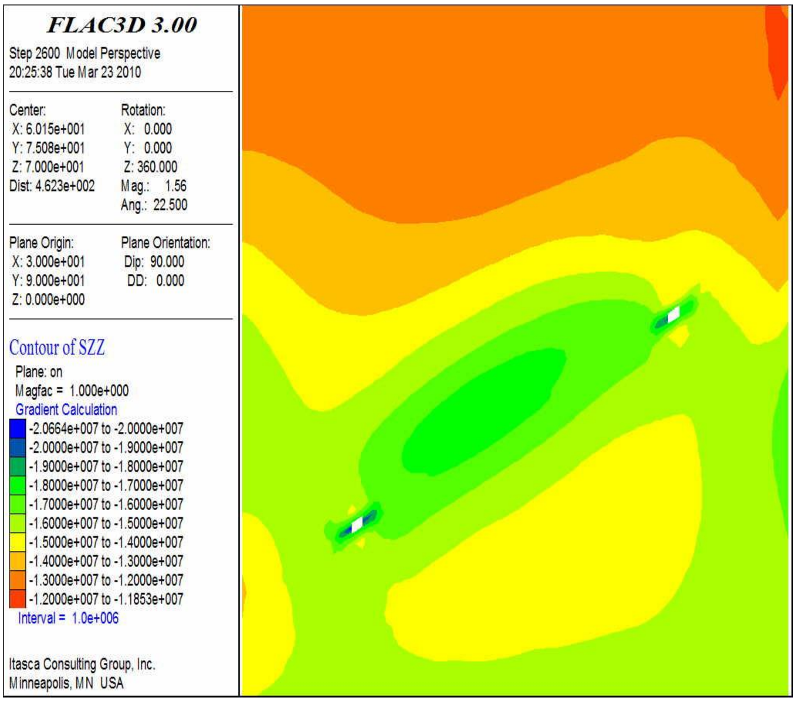

(**a**)

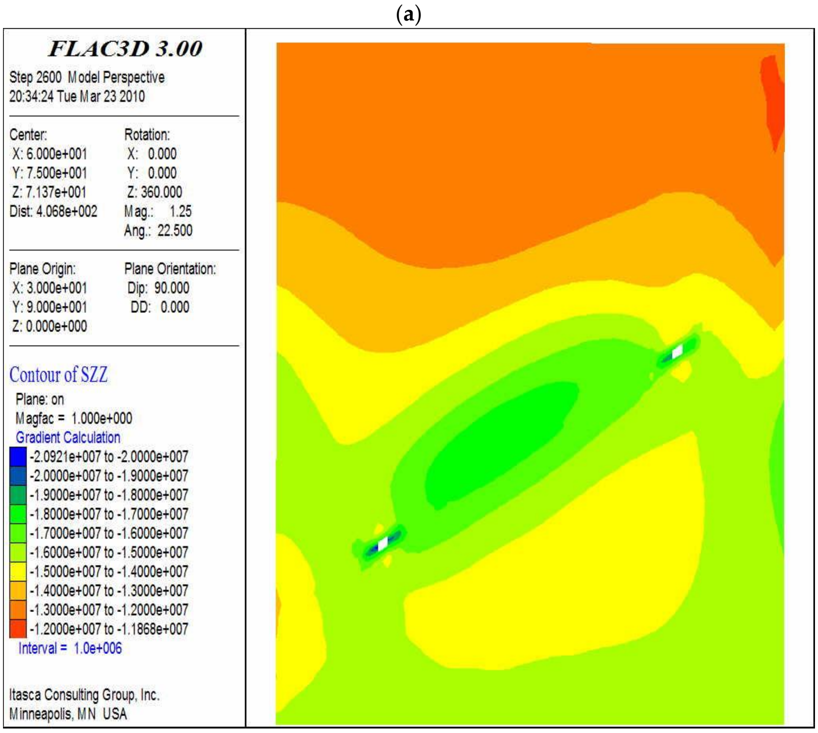

(**b**)

Figure 16. *Cont.*

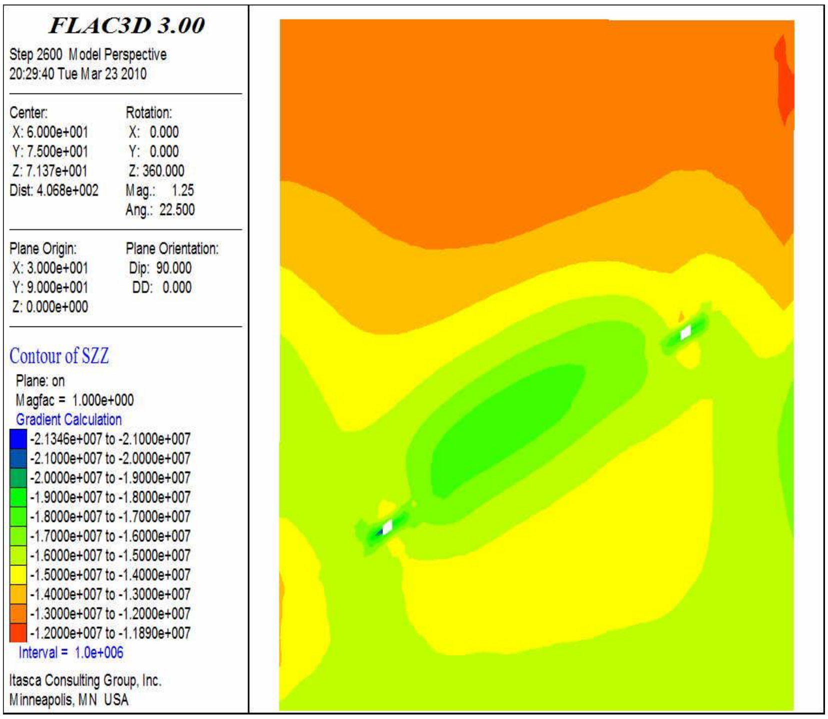

(**c**)

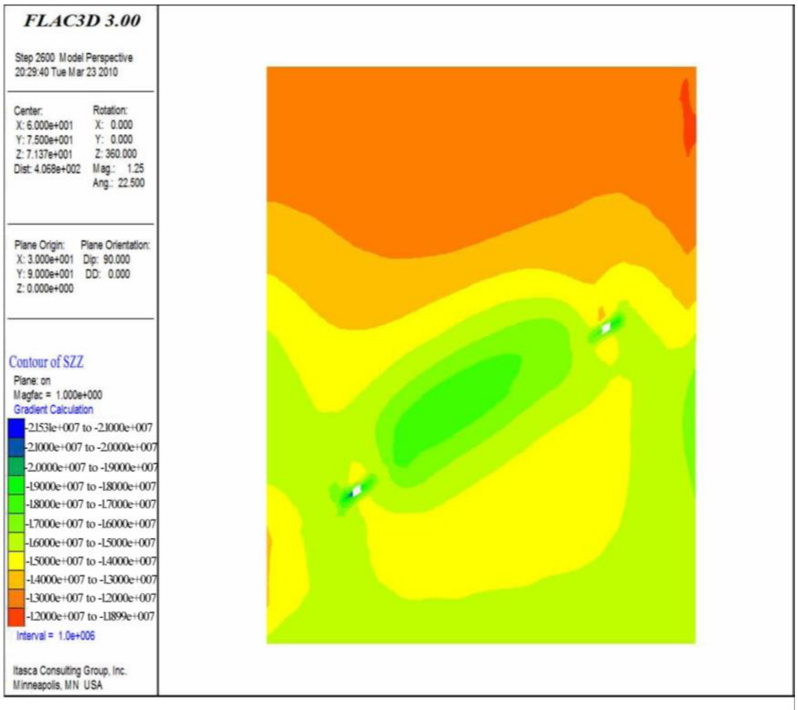

(**d**)

Figure 16. Vertical stress in coal seam after different water injection time: (**a**) 5 h; (**b**) 10 h; (**c**) 15 h and (**d**) 30 h.

The vertical stress of working face on strike before and after water injection are shown in Figure 17. Before water injection, the stress concentration is located on the front area of the plastic zone of the upper and lower roadway and expands about 3–10 m to the sides. The maximum stress is close to the mining face and the stress of the lower roadway is greater than that of the upper one. When the time of water injection reaches 30 h, the maximum stress and stress in the plastic zone obviously decreases and the stress concentration surrounding the water injection hole is generally disappeared. This illustrates that water injection can effectively soften the coal body and release or partially transfer the stresses. This can effectively reduce stress concentration at the working face and the danger of rockbursts.

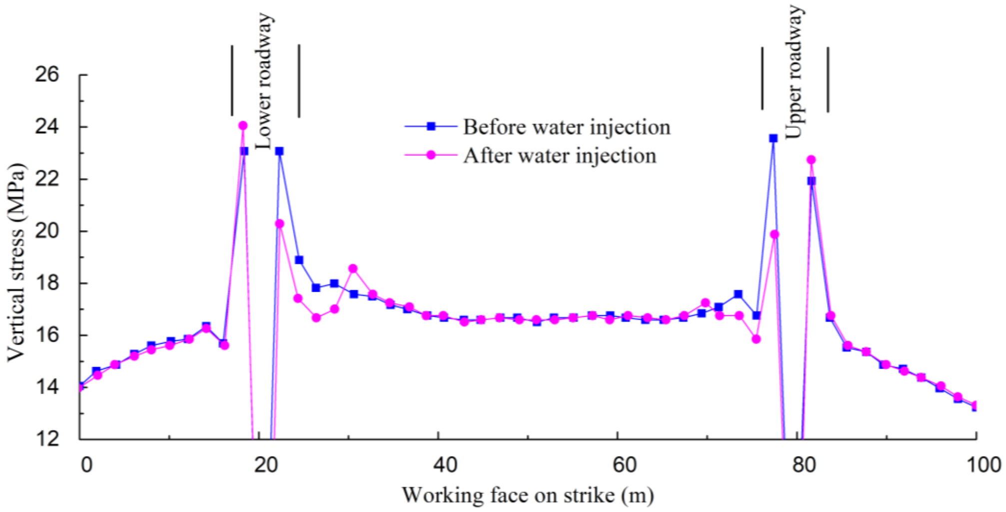

Figure 17. Vertical stress before and after water injection.

4.2. The On-Site Test

The measures of preventing and controlling rockbursts by using water injection were used on another similar working face in the Changgouyu coal mine. Water injection of long borehole length was applied in both upper and lower roadway along the coal seam tendency. Water was injected to the three boreholes at the same time, and circular water injection was used per 10 days. The details of other water injection parameters were shown in Table 8.

Table 8. Parameters of water injection of long borehole length on-site.

Pressurized Method	Drilling Direction of Holes	Borehole Length (m)	Borehole Interval (m)	Sealing Depth (m)	Water Pressure (MPa)	Effective Flow Per Meter Per Hour in Holes ($L \cdot h^{-1}$)
Dynamic pressure	Down	60	15	5–10	9–13	40–50

The water injection effectiveness was tested by the electromagnetic radiation (abbreviated EMR) technology. EMR is related to the stress of the coal and rock mass, and it reflects the stress concentration on the front of the working face. The higher the stress is, the more intense the deformation and fractures of a coal body and the stronger the EMR signals. EMR signals reflect the degrees of concentrated stress of a coal body and danger of a rockburst. The electromagnetic radiation technology can be used to test the effectiveness of stress concentration relieving caused by water injection.

A KBD5 type portable EMR monitor (Fu'an Technology Co., Ltd, Xuzhou, China) was used in the study. The distance between two adjacent EMR testing points in the coal wall or roadway is 10 m and the testing time at each testing point is 2 min [26,27]. EMR intensity (abbreviated E), measured as mV, is selected as the EMR testing index for the stress distribution. EMR methods for predicting rock burst are dynamic and a critical value is used in this method. In general, based on the EMR forecasting criterion, the E value which is 1.5 times the normal E value is selected as the initial critical E value in the monitoring area. After a period of testing and according to the E value before the incidence of a rock burst, the initial critical E value is modified by fuzzy mathematics. After further validation, a critical E value can be confirmed. The critical E value of this working face in the Changgouyu coalmine was determined as 12 mV. During the test process, if the E value of the monitoring area exceeds 15 mV and it appears as a special time trend (the trend is explained in reference [28] in details) over several shifts or days, then a rockburst will likely occur in this monitoring area.

Figure 18 shows that the EMR signals were relatively stable from 1 April 2011 to 5 April 2011, and the strength was less than 10 mV. The E value gradually increased on April 6th and it reached 15 mV on 7 April that was above the critical value. This indicated that the stress at the working face and the lower roadway had increased, and the stress concentration and the danger of strong rock pressure were also increased. Therefore, measures should be taken to reduce such risks.

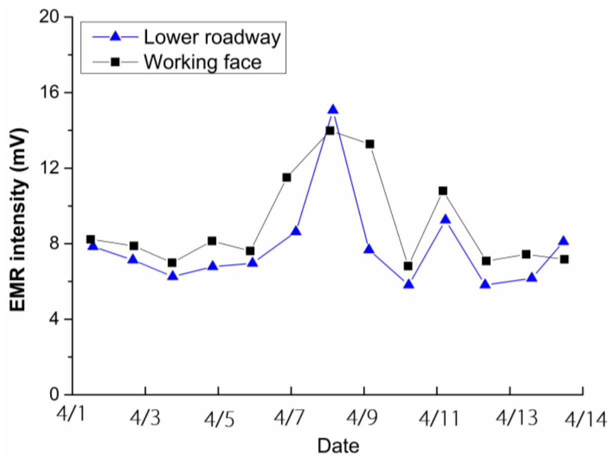

Figure 18. The change of EMR signals at the working face and lower roadway.

From 8 April and the following three days, beyond the circular water injection of long borehole length, the emergent water injection of short borehole length started at the working face and lower roadway. The depth of the borehole was only 10 m, but the number of boreholes was added by 8, 1 and 5 in the three days, and the injection durations is was min, 30 min, and 30 min per day.

After water injection for three days, the EMR intensity at the working face and lower roadway decreased, its value was lower than 10 mV and it became stable again. This illustrated that the water injection is effective. It can effectively soften the coal body and release or transfer the stress. The danger of strong rock stress disappeared.

There was a strong rockburst on 23 May in another coal seam, which caused apparent damage to one of the roadways and the working face. After that, water injection also was used as a preventative action. Although three weak rockbursts happened after that, the damage caused was small. This shows the obvious effect of coal seam water injection on the preventing and controlling of rock stress on-site.

5. Discussion

Coal is a porous medium with a large number of cracks and pores inside. Water flows inside coal in the form of permeation, capillary movement and diffusion. After soaking, water slowly flows along cracks and capillaries. As soaking time increases, the water pressure at crack surfaces and mineral swelling cause changes to the mechanical properties of coal, including an increase of plasticity, and a decline of hardness and compressive strength.

On one hand, water has an expansion effect on the primary cracks of coal. As depicted in Figure 8, the effect changes the pore structure, the number of the cracks and their width. The microstructure surface area increases due to the development of mesostructure. On the other hand, after soaking, water inside samples causes coal body swelling, which not only expands the original crack but also produces new cracks (as shown in Figure 7). As soaking time increases, at the end of the cracks protruding structures develop with a large number of flake structures, and the number and length of cracks increases obviously. Soaking causes a microstructure change, which is determined by soaking time. The surface area and total volume of the internal microstructure of coal samples can be greatly increased by soaking, so it is possible to use water injection to change the the mechanical properties of coal.

After soaking, the mechanical properties of coal have changed. Uniaxial compressive strength, Protodyakonov coefficient and porosity are obviously changed after different soaking times. This demonstrates a time effect. Through studying experimental data, the slope between the relative variation of mechanical parameters of different coal size and soaking time is obtained, as shown in Table 9. The time effect is different for different coal sizes. The obvious effective soaking time in centimeter and millimeter sized coal is the first five days after soaking, but for micron size coal, this is from five to 10 days after soaking.

Table 9. Relationship between mechanical parameters of different size coal and soaking time.

Coal Size	Corresponding Mechanical Parameter	Soaking Duration		
		0–5 Days	5–10 Days	10–15 Days
Centimeter	Reduction of Compressive strength per day (MPa)	2.36	0.63	0.86
Millimeter	Reduction of Protodyakonov coefficient per day (MPa)	0.014	0.078	0.022
Microns	Increment of Porosity per day (%)	0.314	0.316	0.178
	Increment of Total pore volume per day (mL/g)	0.0012	0.0037	0.006
	Increment of Total pore surface area per day (m^2/g)	0.1398	0.2244	0.087

The variation of physical-mechanical parameters of coal in different soaking time is obvious. When the soaking time is 5 days, the decrease of uniaxial compressive strength is the maximum. Although, uniaxial compressive strength continually decreases as soaking time increases, the decrease rate becomes slower at the later stage. There is a change point of pore volume and Protodyakonov coefficient when soaking for five days and 10 days. During this time the decrease rate of the Protodyakonov coefficient and increase of porosity and pore surface area reach the maximum. Based on the analysis, it can be found that the mechanical properties of coal show a time effect during soaking. There is a changing point where mechanical properties of coal are changed dramatically. Therefore, studying the optimal time of coal soaking in the laboratory has an important guiding significance for the on-site application of coal seam water injection.

Bursting liability theory holds that under the same geological and mining conditions, rockbursts in coal seams yield large differences, and their occurrence is determined by the inherent mechanical properties of coal. These inherent properties are regarded as the bursting liability of coal. The so-called bursting liability indices, duration of dynamic fracture (DT), elastic strain energy index (W_{ET}), bursting energy index (K_E), and uniaxial compressive strength (R_C) were proposed to evaluate the bursting liability of coal [29]. Wu et al. [15] concluded that when the moisture content increases by 3%, the uniaxial compressive strength of coal samples reduces by 32%, and there is an exponential relationship between the reduction of coal strength and the immersion time. Pan et al. [21] pointed out that extending the soaking time can reduce the overall degree of burst tendency of coal samples with strong tendency. Uniaxial compressive strength falls rapidly after seven days of soaking, and the degree of the other three indexes begins to increase after 20 days soaking. Mao et al. [18] determined the relationship between the burst liability and water content and porosity in coal seam by experimental studies, and found that the burst liability depends inversely on the water content, and is most sensitive to the original water content. Studies by Liu [16] and Sun [17] applied water injection measures to rockburst prevention in different coal mines. The above studies focused on the mechanic mechanism of water injection on coal on a macro scale (from centimeter to meter size), and the micro scale mechanics mechanism had not been studied.

We analyzed the time effect mechanism of water on different sizes of coal (from meter to nano-meter size). Uniaxial compressive strength, Protodyakonov coefficient and the porosity are measured after the samples have completely soaked in water for a period of time. During soaking, a small amount of hydrophilic mineral absorbs water and swells that cause a decrease of coal strength.

Water is a solvent that can dissolve soluble minerals, and the degree of dissolution is related to soaking time. Because of this, the strength of coal increases, which leads to the burst liability of coal samples changing with soaking time. In the numerical simulation and on-site application, pressurized water is used which is favorable for infiltrating the coal seams, reducing the effective time of water injection and improving efficiency.

Our research had provided a method to study the time effect of water injection on the mechanical properties of coal of different sizes and its application in rockburst prevention. The proposed water injection measure and parameters are only applicable to the Changgouyu coal mine, where the natural water content of its coal is 0.26%, and the average water content exceeds 1.29% after absorption, so the permeability of this coal seam is relatively poor. Further studies are needed for different coal seams with different coal properties

6. Conclusions

(1) The mechanical properties of coal samples under soaking for different durations are tested in the laboratory. The time effect differs with the coal size. When the soaking time was five days, the rate of decrease of uniaxial compressive strength was the maximum. In addition, there was a changing point in the Protodyakonov coefficient, porosity and pore volume and surface area. After soaking for 10 days, the surface area increase of micropore, small pore, mesopore, big pore and visible pores and total surface area of pores reached the maximum.

(2) As soaking time increases, changes to the pores, cracks, bubbles and flake structures inside the coal body take place and develop gradually. When the soaking time is between 10 days and 15 days, the development of the microstructure inside the coal body is sufficient and it shows that the internal skeleton and the mechanical properties of coal are changed.

(3) The numerical simulation results show that the coal body is softened and the stress concentration changes significantly as a result of water injection. As the duration of water injection increases, the stress concentration is gradually released or transferred. When the injection time reaches 30 h, the stress concentration in the water injection area disappears, and the stress in the whole plastic zone also decreases significantly. On-site test results in the Changgouyu coal mine demonstrated that water injection can effectively soften coal bodies and release or transfer stresses, and showed the apparent time effect of water injection on rock prevention and control.

Acknowledgments: This work was supported by the Fundamental Research Funds for the Central Universities (2017CXNL02), and A Project Funded by the Priority Academic Program Development of Jiangsu Higher Education Institutions (PAPD). This work also was funded by China Scholarship Council. The authors are grateful to all the people who help us in this paper.

Author Contributions: For this paper, Xiaofei Liu put forward the study ideas, conducted the on-site tests, and wrote this paper; Guang Xu discussed experimental ideas with Xiaofei Liu and completed a part of the data analysis; the laboratory tests was completed by Dong Zhu and Chong Zhang; the numerical simulation and analysis was completed by Mingyao Wei; the data analysis were by Chong Zhang, Biao Kong and Jifa Qian.

Conflicts of Interest: The authors declare no conflicts of interest.

References

1. Jiang, Y. *Investigation on the Mechanism of Coal Bumps and Relating Experiments*; Press Science: Beijing, China, 2009.
2. Chen, X.; Li, W.; Yan, X. Analysis on rock burst danger when fully mechanized caving coal face passed fault with deep mining. *Saf. Sci.* **2012**, *50*, 645–652. [CrossRef]
3. Jiang, Y.D.; Pan, Y.S.; Jiang, F.X.; Dou, L.M.; Ju, Y. State of the art review on mechanism and prevention of coal bumps in China. *J. China Coal Soc.* **2014**, *39*, 205–213.
4. Cai, M. Principles of rock support in burst-prone ground. *Tunn. Undergr. Space Technol.* **2013**, *36*, 46–56. [CrossRef]
5. Qian, M.; Shi, P. *Mine Pressure and Ground Control*; China University of Mining and Technology Press: Xuzhou, China, 2003; pp. 65–97.
6. Sainoki, A.; Mitri, H.S. Dynamic behavior of mining-induced fault slip. *Int. J. Rock Mech. Min. Sci.* **2014**, *66*, 19–29.

7. Patynska, R.; Kabiesz, J. Scale of seismic and rock burst hazard in the Silesian companies in Poland. *Int. J. Rock Mech. Min. Sci.* **2009**, *19*, 604–608. [CrossRef]
8. Pan, J.; Mao, D.; Lan, H.; Lan, H.; Wang, S.; Qi, Q. Study status and prospects of mine pressure bumping control technology in China. *Coal Sci. Technol.* **2013**, *41*, 21–25.
9. Turner, M.H.; Player, J.R. Seismicity at big bell mine. In *Proceedings Massmin 2000*; The Australasian Institute of Mining and Metalurgy: Melbourne, Australia, 2000; pp. 791–797.
10. Simser, B.; Andrieus, P.; Gaudreau, D. Rockburst support at Noranda's Brunswick mine, Bathurst, New Brunswick. In Proceedings of the 5th North American Rock Mechanics Symposium, Toronto, ON, Canada, 7–10 July 2002; Hammah, R., Bawden, W., Curran, J., Telesnicki, M., Eds.; Volume 1, pp. 805–813.
11. Qi, Q.; Lei, Y.; Li, H.; Ji, Z.; Liu, J.; Pan, J.; Wang, Y. Theory and application of prevention of rock burst by break-tip blast in deep hole. *Chin. J. Rock Mech. Eng.* **2007**, *26*, 3522–3527.
12. Zhang, M.; Song, W.; Pan, Y. Study on Water Pouring into Coal Seam to Prevent Rock-burst. *J. Saf. Sci. Technol.* **2003**, *13*, 69–72.
13. Lan, Y. *The Study on Drillhole Pressure Relief Preventing Rockburst in Coal Mine*; Liaoning Technology University: Fuxin, China, 2004.
14. Huang, B.; Cheng, Q.; Liu, C.; Wei, M.; Fu, J. Hydraulic Fracturing Theory of Coal-Rock Mass and Its Technical Framework. *J. Min. Saf. Eng.* **2011**, *28*, 167–173.
15. Wu, Y.; Wang, S.; Zhang, W. Discussion on mechanism of rockburst prevention by water infusion. *J. China Coal Soc.* **1989**, *2*, 69–80.
16. Liu, S.; Li, G.; Pan, J.; Ding, S. Technology of Rock-burst Prevention by Water-injection in 1000 m Buried Coal-seam. *Coal Min. Technol.* **2011**, *16*, 76–78.
17. Sun, H.; Xu, L.; Zhu, F.; Mao, X.; Miao, X. The prevention and control of water injection method for soft rock mine rockburst accident. *Coal Sci. Technol.* **1999**, *27*, 48–50.
18. Mao, X.; Chen, Z.; Xu, S.; Li, T. Experimental study on the relation between the burst tendency and water content in coal seam. *Chin. J. Rock Mech. Eng.* **2001**, *20*, 49–52.
19. Feng, Z.; Zhao, Y. Correlativity of rock inhomogeneity and rock burst trend. *Chin. J. Rock Mech. Eng.* **2003**, *22*, 1863–1865.
20. Shi, B.; Mu, C. Experiment Study on Water Injection and Moist Role for Outburst Prevention of Outburst Sea. *Coal Sci. Technol.* **2013**, *41*, 147–150.
21. Pan, J.F.; Ning, Y.; Lan, H.; Peng, Y.-W.; Xia, Y.-X.; Wei, X.-Z.; Wang, S.-W. Water injection methods in coal bed based on experiments of water immersion time effect of Qianqiu coal samples with burst trend. *J. China Coal Soc.* **2012**, *37*, 19–25.
22. Kang, T. The Study of permeability and classication on infusion in coal seam. *Chin. J. Rock Mech. Eng.* **1995**, *14*, 260–268.
23. Yetkin, M.E.; Kahraman, B.; Özfırat, M.K.; Şengün, B.; Şimşir, F. Determination of travertine samples porosity using image analysis method. *Indian J. Eng.* **2017**, *37*, 227–235.
24. Zou, M.; Wei, C.; Zhang, M.; Shen, J.; Chen, Y.; Qi, Y. Classifying coal pores and estimating reservoir parameters by nuclear magnetic resonance and mercury intrusion porosimetry. *Energy Fuels* **2013**, *27*, 3699–3708. [CrossRef]
25. Mallı, T.; Yetkin, M.E.; Özfırat, M.K.; Kahraman, B. Numerical analysis of underground space and pillar design in metalliferous mine. *J. Afr. Earth Sci.* **2017**, *134*, 365–372. [CrossRef]
26. Wang, E.; He, X.; Liu, X.; Li, Z.; Wang, C.; Xiao, D. A non-contact mine pressure evaluation method by electromagnetic radiation. *J. Appl. Geophys.* **2011**, *75*, 338–344. [CrossRef]
27. He, X.; Chen, W.; Nie, B.; Mitri, H. Electromagnetic emission theory and its application dynamic phenomena in coal-rock. *Int. J. Rock Mech. Min. Sci.* **2011**, *48*, 1352–1358. [CrossRef]
28. Wang, E.; Liu, X.; Zhao, E.; Liu, Z. Study of electromagnetic characteristics of stress distribution and sudden changes in the mining of gob-surrounded coal face. *J. China Univ. Min. Technol.* **2008**, *18*, 1–5. [CrossRef]
29. Liu, X.; Wang, X.; Wang, E.; Kong, X.; Zhang, C.; Liu, S.; Zhao, E. Effects of gas pressure on bursting liability of coal under uniaxial conditions. *J. Nat. Gas Sci. Eng.* **2017**, *39*, 90–100. [CrossRef]